Introductory Overview of Superconducting RF Technology

Kenneth Shepard
ANL Physics Division

Beams and Applications Seminar

June 1, 2007

Argonne NATIONAL LABORATORY

... for a brighter future

U.S. Department of Energy

UChicago Argonne LLC

Office of Science U.S. DEPARTMENT OF ENERGY

A U.S. Department of Energy laboratory managed by UChicago Argonne, LLC

Outline

- Most of my career has been developing superconducting cavities for accelerating ion beams – reduced velocity structures – but RFSC technology is much the same for all SC structures

- This overview will be primarily technical rather than historical
  - Fundamental properties of SC at high frequencies and high fields
  - Elements of constructing, processing, and operating SC cavities
  - Can we say anything useful about where the technology goes from here?

- This is the first of three seminars on Superconducting RF (SRF) technology:

  June 8 - Mike Kelly will discuss surface processing and cavity performance

  June 15 - Zach Conway will discuss couplers, tuners, and the electromechanical properties of SC cavities

Kamerlingh Onnes and Johannes Van der Waals with the 1st Helium Liquifier, Leiden ca. 1910

- 1911 - superconductivity discovered by Kamerlingh Onnes
- 1930's:
  - magnetic flux expulsion discovered by Meissner & Ochsenfeld
  - London equations (zero momentum state)
- 1950's:
  - Ginsburg/Landau theory developed – (Abrikosov vortices)
  - Pippard: non-local electrodynamics
  - 1957 – Bardeen, Cooper, & Schrieffer theory
- Theoretical understanding opened the way for applications (SC magnets, quantized flux magnetometry, etc.)
- 1964 – SC cavities developed for accelerator applications at Stanford (I started grad school there)

Meissner Effect – the phase transition to the SC state

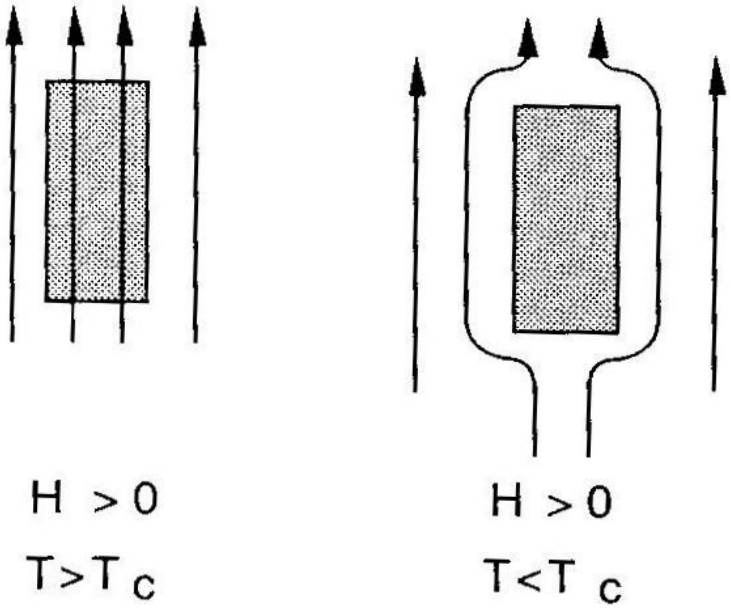

The magnetic field penetrates into the SC a distance λ ≈ 500Å for nb (the penetration depth)

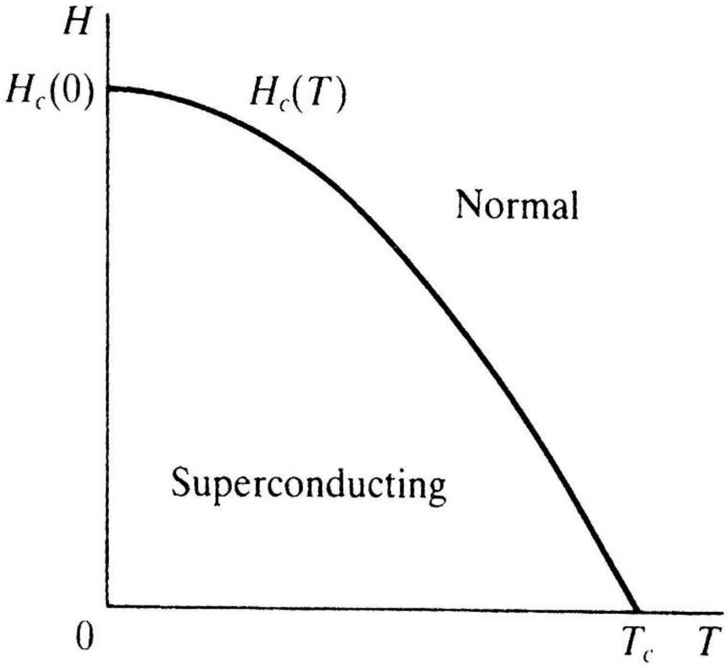

In zero magnetic field, the phase transition is 2nd order (no latent heat). In a finite external field the transition is 1st order.

Penetration depth – Coherence Length

Boundary between SC and Normal regions in a metal

$\lambda(T) \approx \lambda_0/(1-T^4/T_C^4)^{1/2}$

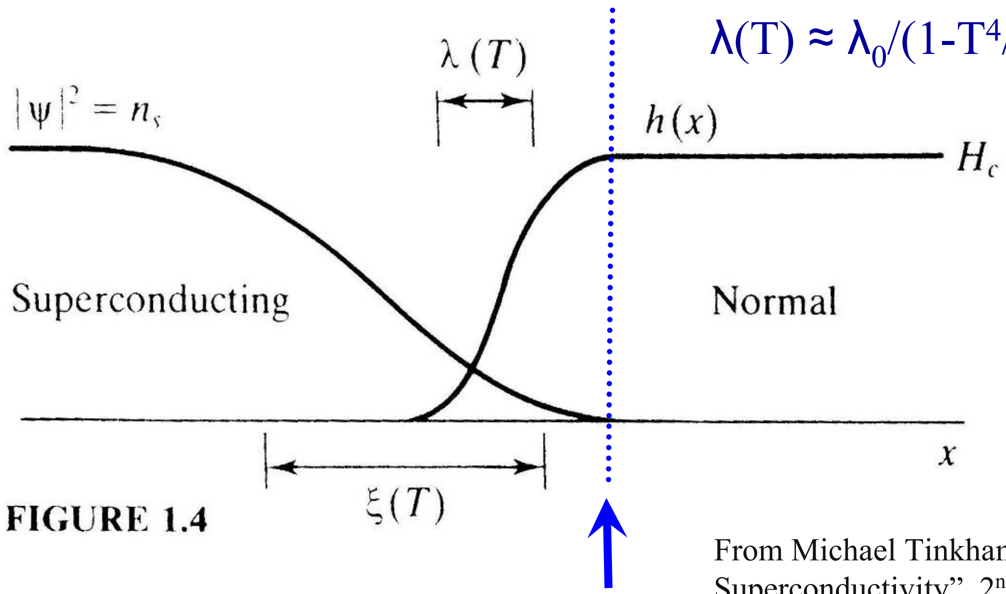

FIGURE 1.4

From Michael Tinkham's "Introduction to Superconductivity", 2nd edition

G-L parameter $\kappa = \lambda/\varepsilon$

for $\kappa < 1/\sqrt{2}$, surface energy is positive (type I SC)

for $\kappa > 1/\sqrt{2}$, surface energy is negative (type II SC)
Magnetic flux breaks into the smallest possible units which are flux-tubes or vortices containing a single quantum of magnetic flux $\Phi0 = h/2e = 2 \bullet 10^{-15}$ W

For niobium:
λ_0 = 500 Å
ε_0 = 300 Å
κ = 1.66

Type II Superconductors exhibit a mixed state in an external field

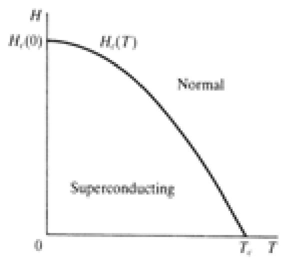

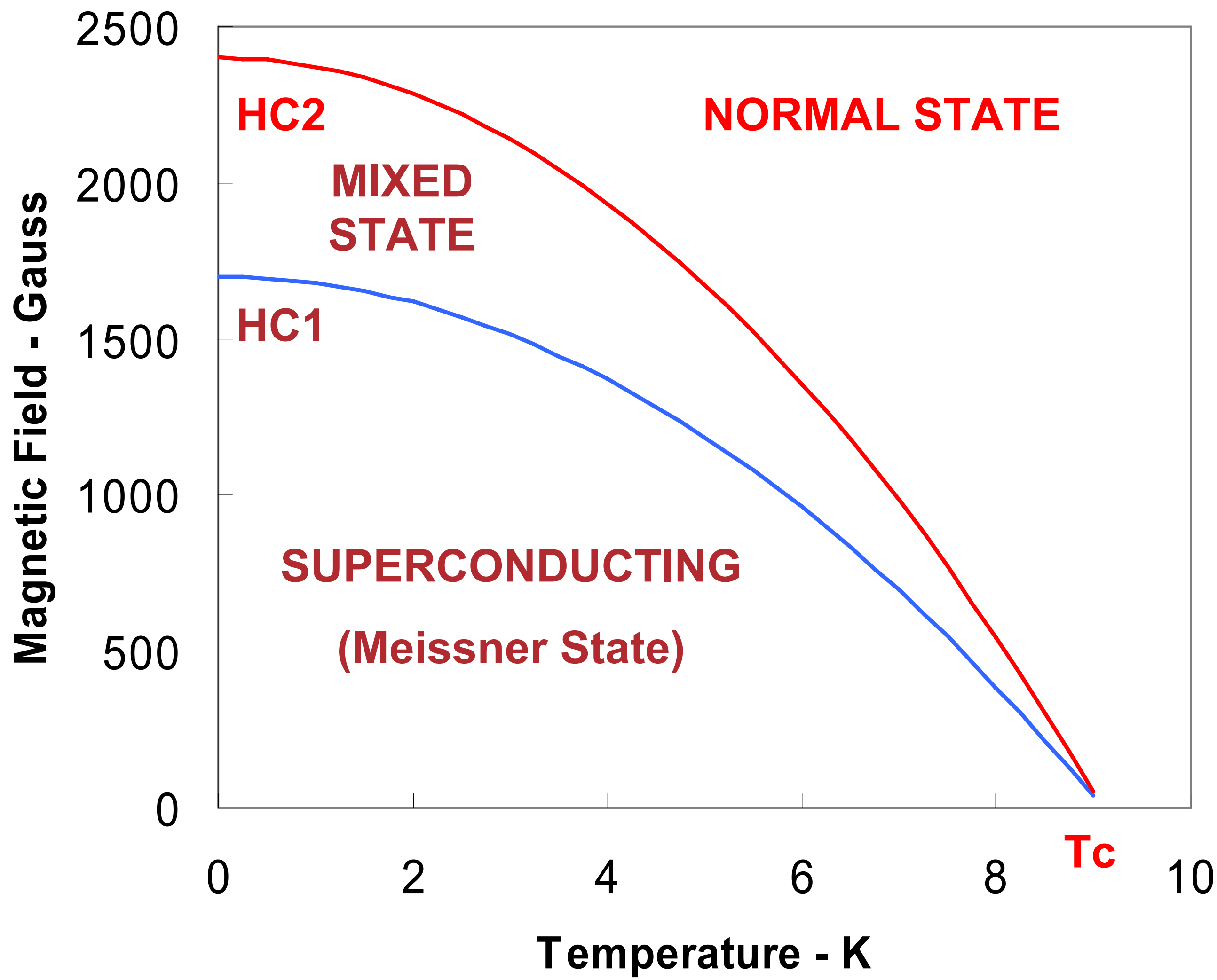

$H_{C2} = \sqrt{2} \bullet \kappa \bullet H_C$

SC Materials and Applications

DC Applications (Magnets): Type II, Mixed State

RF Applications (Cavities): Type I or II, Meissner State

Magnetization Curve for Type I and Type II superconductors

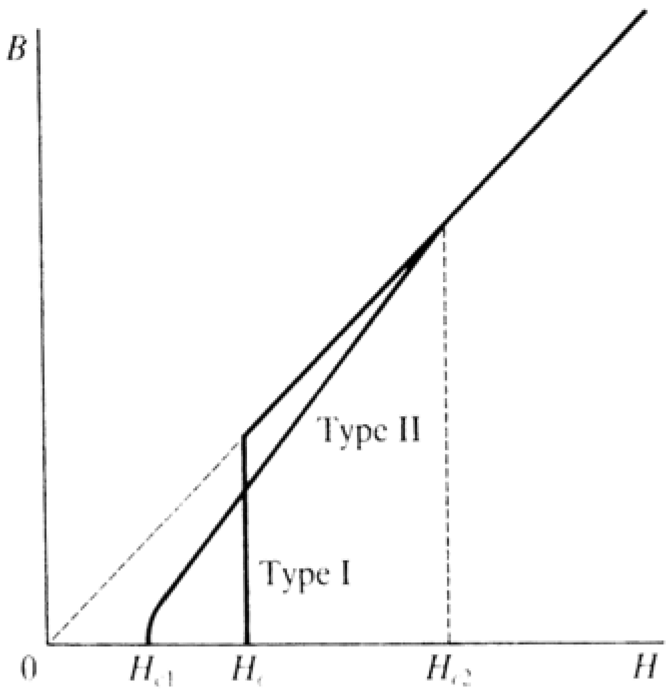

$$H_{C2} = \sqrt{2} \cdot \kappa \cdot H_C$$

Metal	T_C	H_{C1}	H_C	H_{C2}
Pb	7.2 K	*	803 G	*
Nb	9.2K	1700 G	1950 G	3400 G
Nb_3Sn	18 K	380 G	5200 G	25,000 G
YBCO	95 K	**	12000 G	10^6 G **

* Type I superconductor

** Extreme Type II

High-frequency devices have been developed using these superconducting materials

Superconducting State

- Electrons form Cooper-pairs through weak attractive interaction
- Electron pairs (bosons) condense into zero-momentum state where: **p** = (m·**v** + e·**A**/c) = 0
- Conduction electrons can be described by a two-fluid model of the condensate (superconducting electrons) and excitations (normal electrons)
- The behavior of the condensate (superfluid) can be described by G-L theory

$$\frac{1}{2m^*}\left(\frac{\hbar}{i}\nabla - \frac{e^*}{c}A\right)^2 \psi + \beta|\psi|^2 \psi = -\alpha(T)\psi$$

- Processes involving the excitations (normal fluid) are central to upper limits of EM fields and power dissipation which are critical to dc and rf applications

RF Losses in Normal metals – normal and anomalous skin effect

- RF currents are confined to a surface layer of thickness $\delta = \sqrt{2/\mu_0 \cdot \omega \cdot \sigma}$
- Giving an effective surface resistance of $R_S = 1/\sigma \cdot \delta = \sqrt{\boldsymbol{\mu_0 \cdot \omega / 2 \cdot \sigma}}$ (ohms/square)
- Power Loss into metal surface is: $\mathbf{P = \frac{1}{2} R_S \cdot H_0^2}$ w/m^2

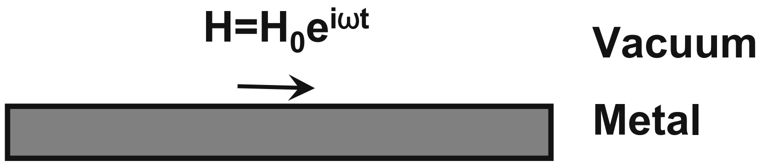

Skin Depth and Surface Resistance at 1.0 GHz			
T		**Cu**	**Nb**
293 K	Skin Depth	2.1 μ	6.1 μ
	Surface Resistance	$8.2 \bullet 10^{-3}$ Ω/sq	$23 \bullet 10^{-3}$ Ω/sq
~ 30 K	Skin Depth	0.2 μ	1.7 μ
	Surface Resistance	$7.9 \bullet 10^{-4}$ Ω/sq	$6.3 \bullet 10^{-3}$ Ω/sq

PHYSICAL REVIEW VOLUME 171, NUMBER 2 10 JULY 1968

Complex Radio-Frequency Impedance of Type-II Superconductors*

George E. Possin† and Kenneth W. Shepard†
Department of Physics, Stanford University, Stanford, California
(Received 17 November 1967)

obey the London equations. Assuming $\exp(i\omega t)$ time dependence,

$$i\omega(4\pi\lambda^2/c^2)\mathbf{J}_s=\mathbf{E}, \tag{7}$$

$$\mathbf{J}=\mathbf{J}_s+\mathbf{J}_n, \tag{8}$$

$$\mathbf{J}_n=(n_n/n)\sigma_n\mathbf{E}, \tag{9}$$

where $\mathbf{J}_n$ and $\mathbf{J}_s$ are the normal and superconducting current densities, λ is the penetration depth, n is the total electron density, and n_n is the normal electron density. Assuming the usual slab geometry we can solve the above equations for the impedance Z:

$$Z=V/I=l\,|\mathbf{E}|/wd\,|\mathbf{J}| \tag{10}$$

or

$$Z=(1/R+1/i\omega L)^{-1}\cong\omega^2L^2/R+i\omega L, \tag{11}$$

where we have assumed the usual case of $R_{\mathrm{norm}}\gg\omega L(T)$ and we have taken

$$L=(l/wd)4\pi\lambda^2/c^2 \tag{12}$$

and

$$R=(l/wd)n/n_n\sigma_n. \tag{13}$$

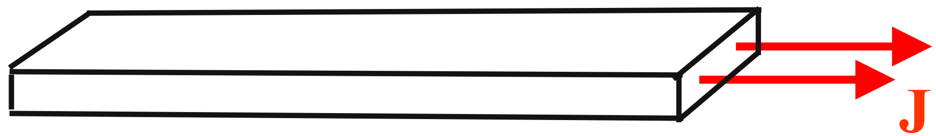

50Å × 2μ aluminum film is a quasi-one-dimensional SC system - the current density is uniform over the cross-section of the strip

A two-fluid model describes the RF impedance:

Voltage across strip: $V \sim J\bullet\omega\bullet L$

Power loss $\sim V^2/R \sim J^2\bullet\omega^2\bullet L^2/R$

The superconducting surface resistance:

1. scales as ω^2
2. Increases rapidly as $T\rightarrow T_C$

SC RF Surface Resistance vs. Frequency

$$R_S = Const \bullet (1/T) \bullet \omega^2 \bullet \exp(-\Delta(T)/kT) + R_0$$

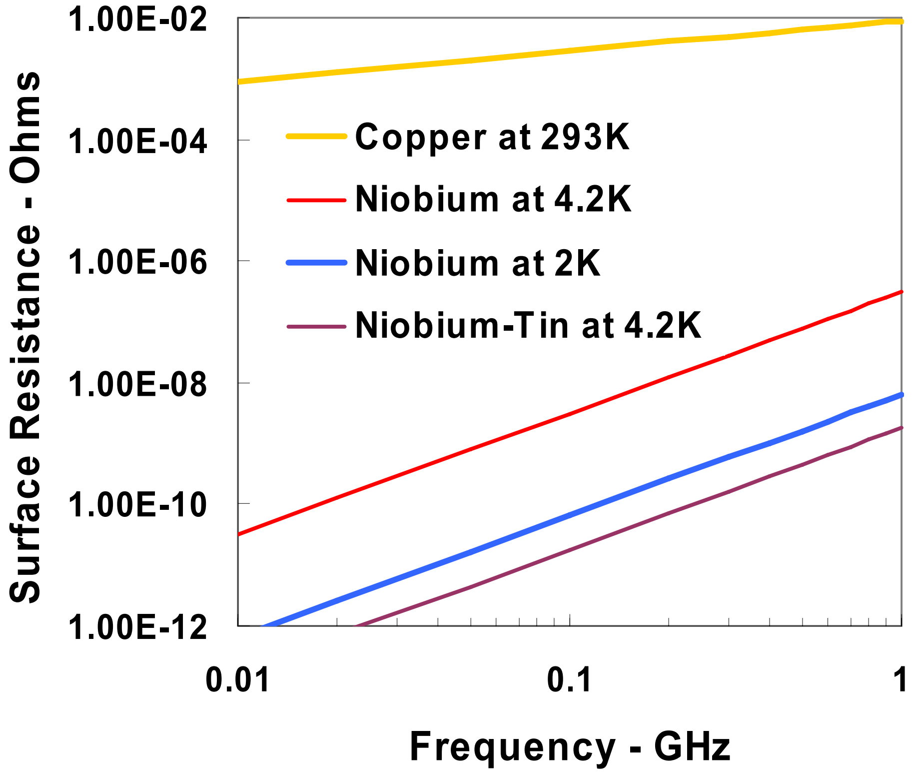

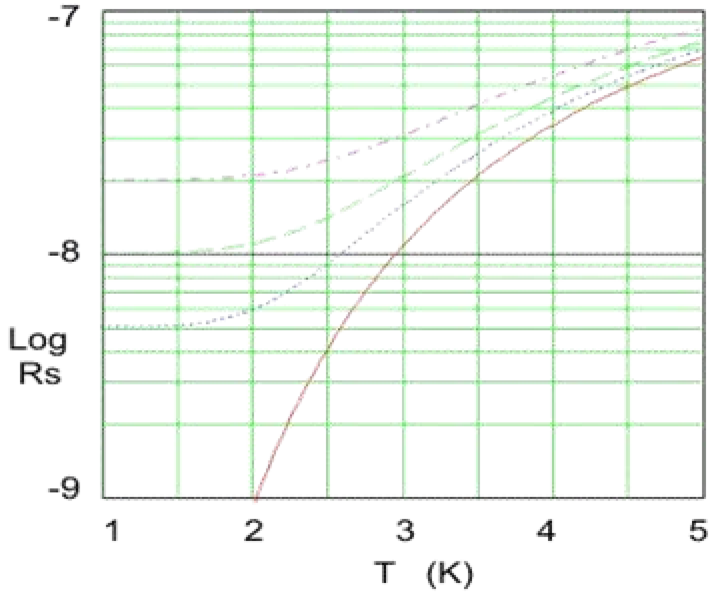

R_s vs. Temperature at 345 MHz for 0, 5, 10, 20 nΩ residual resistivity

SC thin film with in a perpendicular magnetic field

- Lorenz force = J x ϕ_0 on the vortices causes “flux flow” and power dissipation
- For DC applications, vortices must be pinned on defects

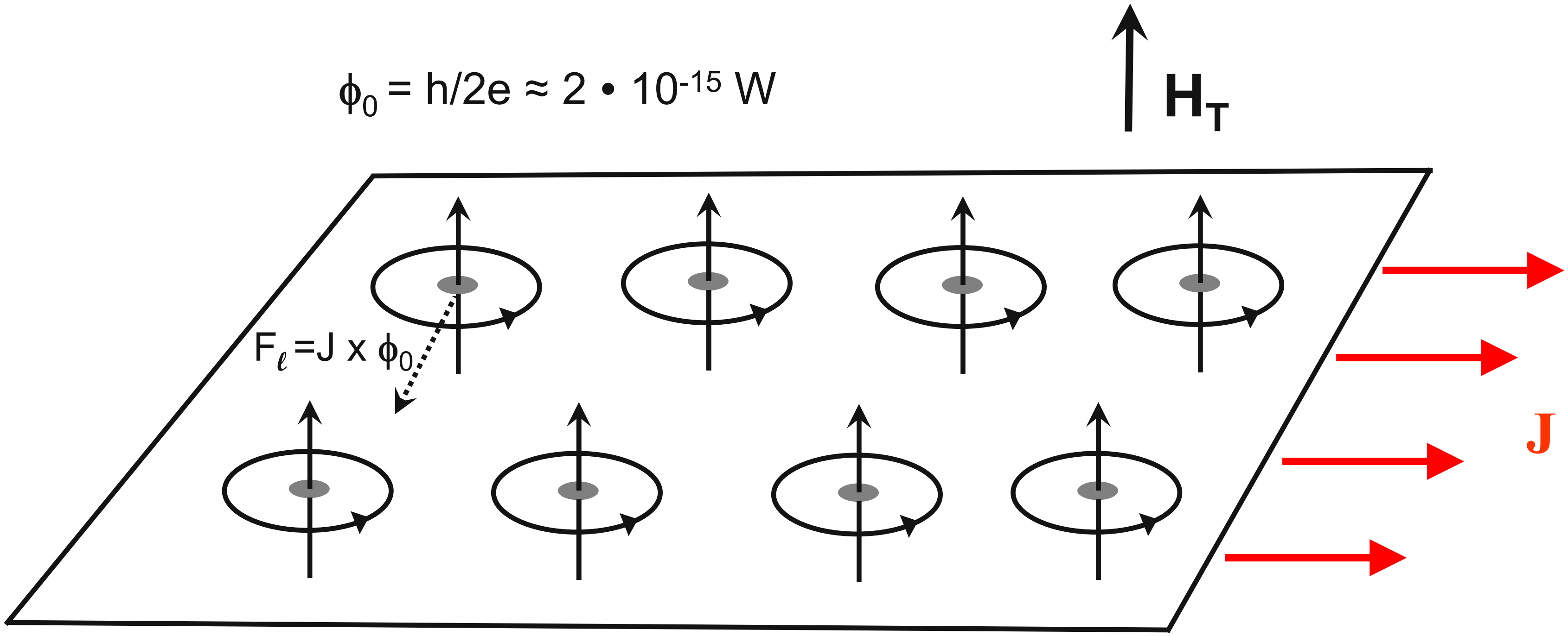

- For RF applications even pinned vortices wiggle about pinning site and cause losses
- R_S(trapped flux) ≈ R_S(anomalous)·(H_T/H_{C2}) ≈ 0.3 nΩ/mG

SC Surface Resistance
Penetration Depth – Skin Depth - Dispersion

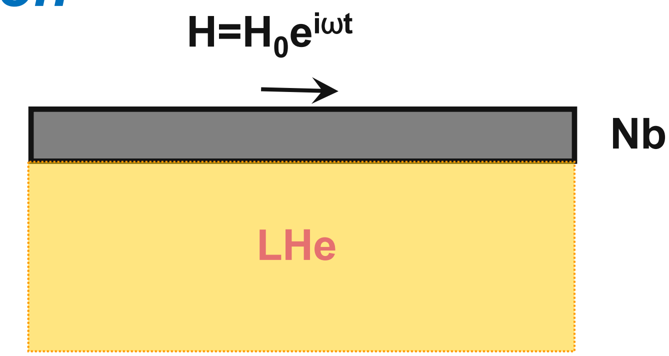

- SC surface resistance is lower by 3-5 orders of magnitude
- Penetration depth does not vary appreciably with frequency
- The maximum SC rf field is $H \leq H_{SH} \approx H_C$

Skin Depth and Surface Resistance at 1.0 GHz			
T		**Cu**	**Nb**
293 K	**Skin Depth**	**2.1 μ**	**6.1 μ**
	Surface Resistance	**$8.2 \cdot 10^{-3}$ Ω/sq**	**$23 \cdot 10^{-3}$ Ω/sq**
~ 30 K	**Skin Depth**	**0.2 μ**	**1.7 μ**
	Surface Resistance	**$7.9 \cdot 10^{-4}$ Ω/sq**	**$6.3 \cdot 10^{-3}$ Ω/sq**
4.2 K	**Penetration Depth**	**0.2 μ**	**0.05 μ**
	Surface Resistance	**$7.9 \cdot 10^{-4}$ Ω/sq**	**$3.2 \cdot 10^{-7}$ Ω/sq**
~ 2 K	**Penetration Depth**	**0.2 μ**	**0.05 μ**
	Surface Resistance	**$7.9 \cdot 10^{-4}$ Ω/sq**	**$6.5 \cdot 10^{-9}$ Ω/sq**

Refrigerator Capital Cost Data

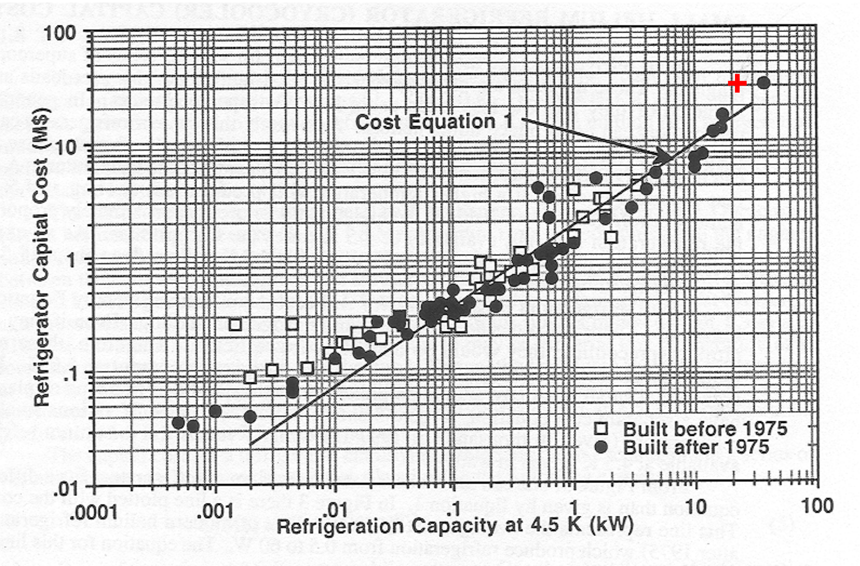

Figure 2. The Cost of Helium Refrigerators versus Refrigeration at 4.5 K.

Byrns, R.A. & Green, M.A., "An update on estimating the cost of cryogenic refrigeration," Advances in Cryogenic Engineering 43, p.1661 (1998)

$$C[M\$_{1997}] = 1.77(R[kW])^{0.7} \qquad (1)$$

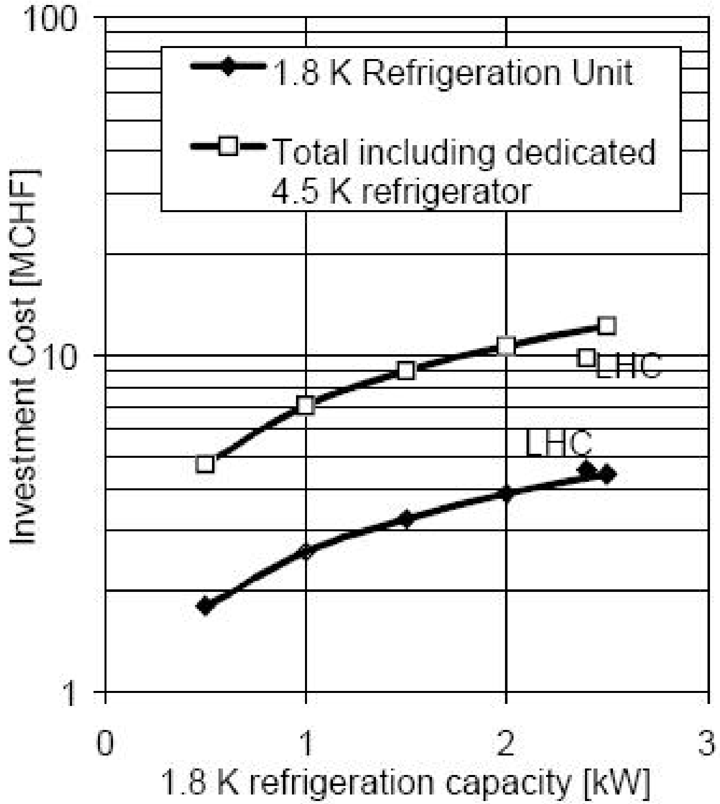

Claudet et al, "Economics of Large Helium Cryogenic Systems: Experience from Recent Projects at CERN," CEC1999

1998 avg exchange rate 1 CHF = 0.7 USD

Refrigerator Operating Costs: Wall-plug power

- Assume capital cost scales with input power (V. Ganni)

- Refrigeration @4.3K:
  - Carnot efficiency = 30%
  - Input power required = 230 W per watt at 4.3K

- Refrigeration @2K:
  - Carnot efficiency = 18%
  - Input power required = 830 W per watt at 2K

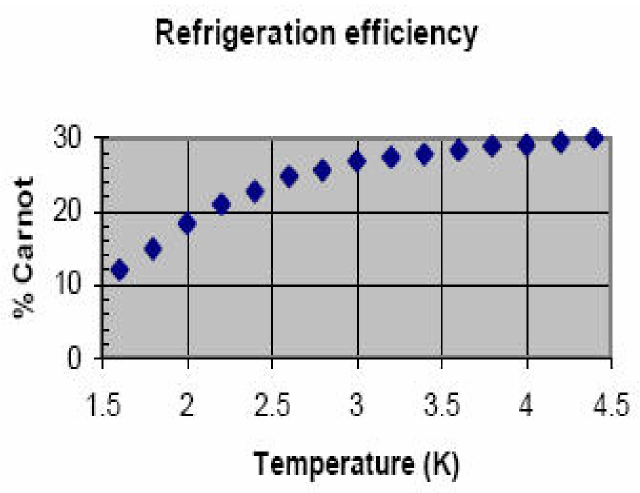

Schneider, Kneisel, Rode, "Gradient Optimization for SC CW Accelerators," PAC2003

What materials have been used and why?

Metal	T_C	H_{C1}	H_C	H_{C2}
Pb	7.2 K	*	803 G	*
Nb	9.2K	1700 G	1950 G	3400 G
Nb_3Sn	18 K	380 G	5200 G	25,000 G
YBCO	95 K	**	12000 G	10^6 G **

- Pb plated on copper - small ion linacs
- Nb sputtered on copper - (CERN, INFN Legnaro)
- High-purity sheet niobium - current state of the art
- YBCO, etc. - only for low-field, low dispersion rf strip-lines and filters

Summarize to this point:

- Depending on frequency and temperature we can reduce RF losses by a factor of 10^4 to 10^6 by going from room temperature copper to niobium at 2-4 K.
- Given the efficiency of present refrigerators, the net wall-plug power savings can be in the range 30 – 1000

- So the game may be worthwhile, but what are the ancillary problems?
  - Field limits and breakdowns: non-linear behavior (Mike Kelly will talk about surface processing and performance next week).
  - Detuning and microphonics (Zach Conway will talk about the issues with phase control in SC cavities in two weeks).

- For the rest of this talk, we will review some of the basic features of cavities, SC cavities, and the nomenclature used in SRF.

An RF Cavity is a hole in a chunk of metal…

Based on transmission-line-like element

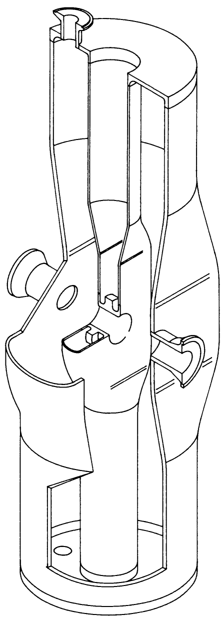

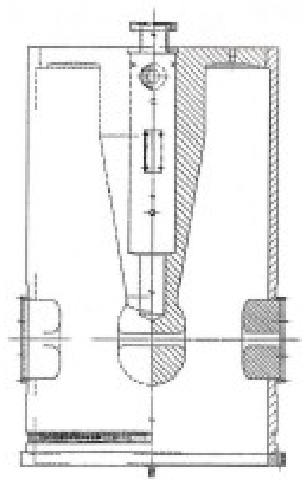

TEM-Class

Based on cylindrical cavity in TM010 mode

TM-Class

Features of TEM and TM Structures

TEM exhibit higher shunt impedence

TEM (spoke) are ½ the diameter at a given frequency

TEM has lower E_{PEAK} for $\beta < 0.5 - 0.6$

TM have lower E_{PEAK} for $\beta > 0.5 - 0.6$

TM have very large aperture

TM generally have lower B_{PEAK}

115 MHz QWR Cavity

Axial electric field in the λ/4 mode

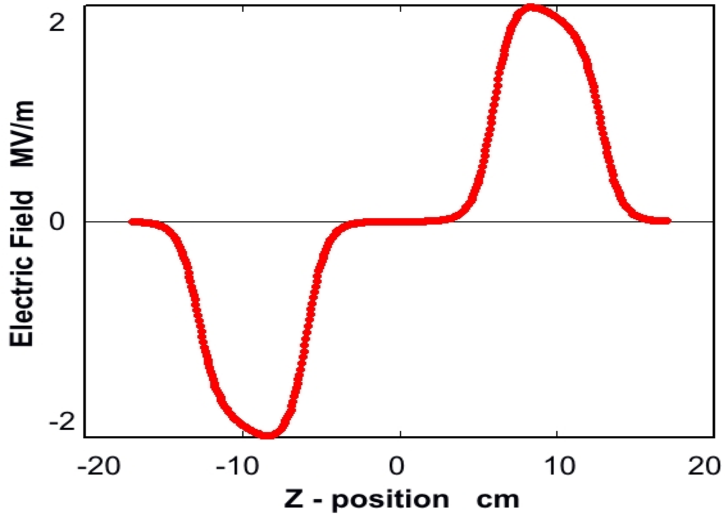

Velocity acceptance (transit-time factor)

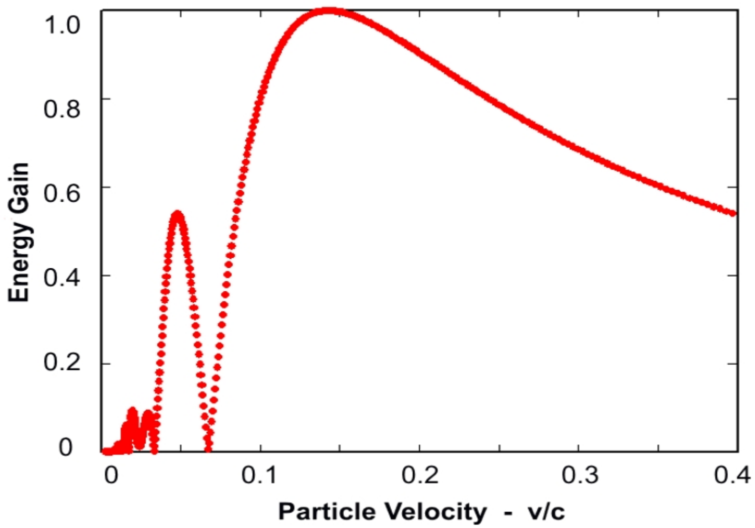

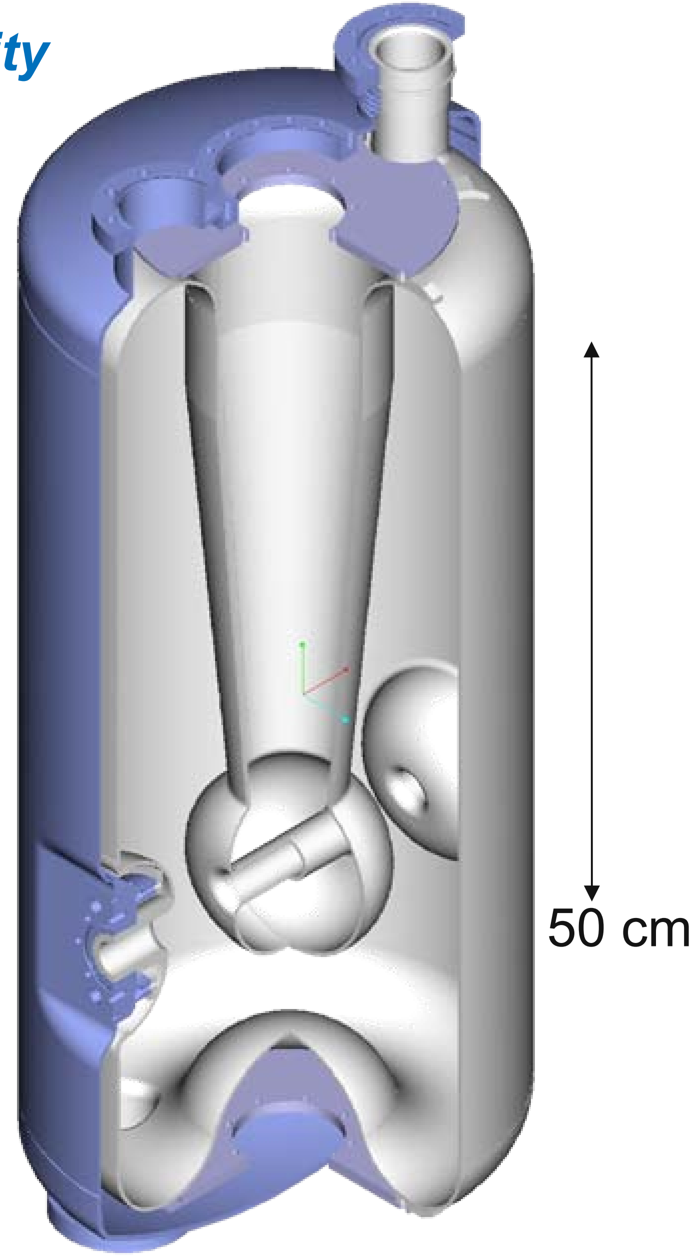

Cavity parameters all refer to a single eigenmode - the accelerating eigenmode of the cavity

- $\boldsymbol{\omega}$ = resonant frequency of the cavity
- $\boldsymbol{l_0}$ = effective length of the cavity (= n·β·λ/2)
- $\mathbf{E_A}$ = the accelerating gradient: the energy gain per unit charge for a synchronous particle divided by the effective length of the cavity
- $\mathbf{U_0}$ = electromagnetic energy content of the cavity at E_{ACC} = 1.0 MV/meter: in general $\mathbf{U(E_A) = U_0 \cdot E_A^2}$
- **Q** = ω/δω = ω·τ where δω = the 3 db cavity bandwidth and τ = the decay time for rf energy in the cavity (rf power P = (rf energy)/τ)

Cavity parameters - continued

- $\mathbf{Q} = \omega/\delta\omega = \omega\cdot\tau$ where $\delta\omega$ = the 3 db cavity bandwidth and τ = the decay time for rf energy in the cavity (rf power $P = (\text{rf energy})/\tau$)

- $\mathbf{G = Q\cdot R_S}$ = the geometric factor for the cavity relates the cavity Q to the rf surface resistance of the cavity

- $\mathbf{Z_{SHUNT}}$ (sometimes labeled as R or R_S) is defined by $\mathbf{P = V^2/ Z_{SHUNT}}$ and is usually given in the form Z_{SHUNT}/Q or **R/Q** we notice that $\mathbf{R/Q = \mathit{l}_0^2/ \omega\cdot U_0}$

- $\mathbf{E_{PEAK}/E_A}$ and $\mathbf{B_{PEAK}/E_A}$ are the ratios of the peak surface fields to the accelerating gradient

We note that the rf power input to a cavity at a gradient $\mathbf{E_{ACC}}$ will be given by:

$$\mathbf{P = G\cdot(\mathit{l}_0\cdot E_A)^2/(R_S\cdot(R/Q))}$$

From: PR-ST AB 8, 042003 (2005), "Prototyping of a multicell sc cavity for acceleration of medium-velocity beams", CC. Compton, et al. (MSU & JLAB)

805 MHz, 6-cell elliptical-cell niobium cavity developed for RIA – high intensity ion beams at β ≈ 1/2

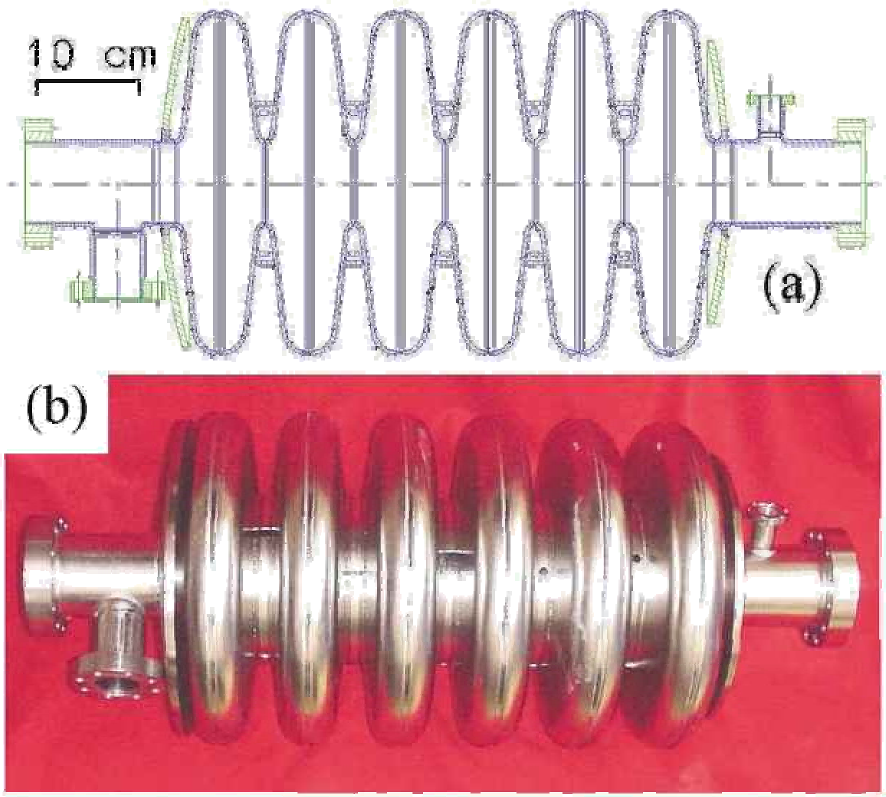

FIG. 5. (Color) (a) Drawing of the second and third 6-cell $\beta_g = 0.47$ Nb cavities and (b) photograph of the second cavity. The port for the input coupler can be seen on the left beam tube. Rings are welded around the outside of the irises to increase the mechanical stiffness of the structure. The end dishes for the attachment of the helium vessel are also visible.

Measured axial electric field – tune for field flatness

Bead pull measures magnitude E^2 along the beam axis

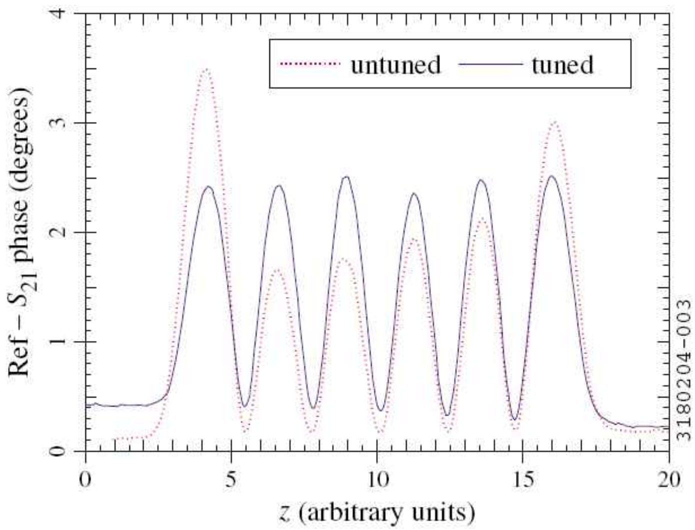

FIG. 6. (Color) Bead pulls for the second 6-cell niobium cavity. The phase shift (proportional to the square of the electric field) as a function of bead position z was measured with a network analyzer.

Transit-time factor shows the effects of adding cells to the cavity

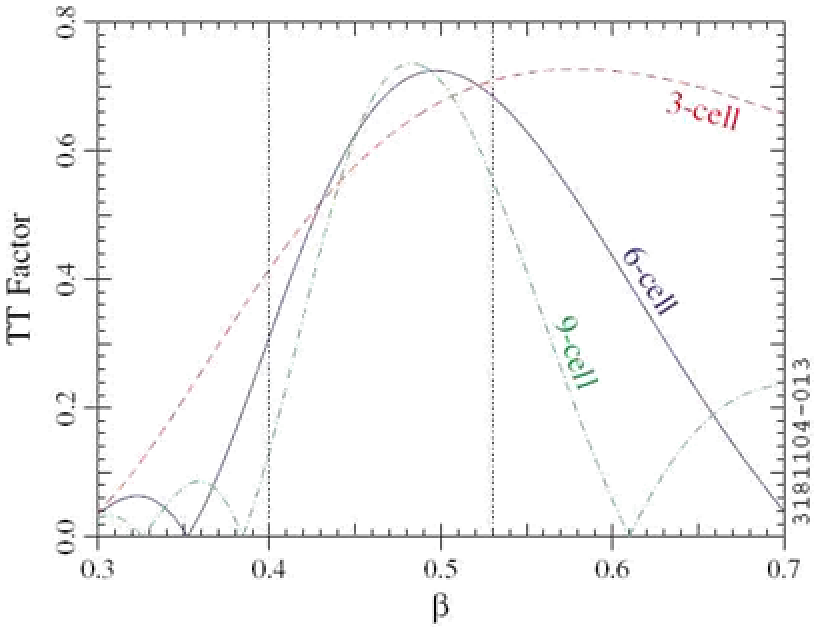

FIG. 2. (Color) Dependence of the transit time factor on β for the $\beta_g = 0.47$ cavity for 3, 6, and 9 cells.

042003-3

6-cell cavity parameters

TABLE I. Parameters of the symmetric 6-cell $\beta_g = 0.47$ cavity. The rf quantities were calculated with SUPERFISH.

Cell mode	TM_{010}
Phase advance per cell	π
Resonant frequency f	805 MHz
Cell-to-cell coupling $\equiv 2(f_\pi - f_0)/(f_\pi + f_0)$	1.5%
E_p/E_a	3.34
cB_p/E_a	1.98
R_a/Q	173 Ω
Geometry factor G	136 Ω
Active length $\equiv 6\beta_g c/(2f)$	527 mm
Inner diameter at iris (aperture)	77.2 mm
Inner diameter at equator	329 mm

$U_0 = 0.635\ \mathrm{J/(MV/m)^2}$

$B_P/E_A = 66\ \mathrm{G/(MV/m)}$

What do the Q-curves tell us?

At 10 MV/m and 2K, the rf power input is

16 watts (into 2K helium)

The stored rf energy is 63.5 joules

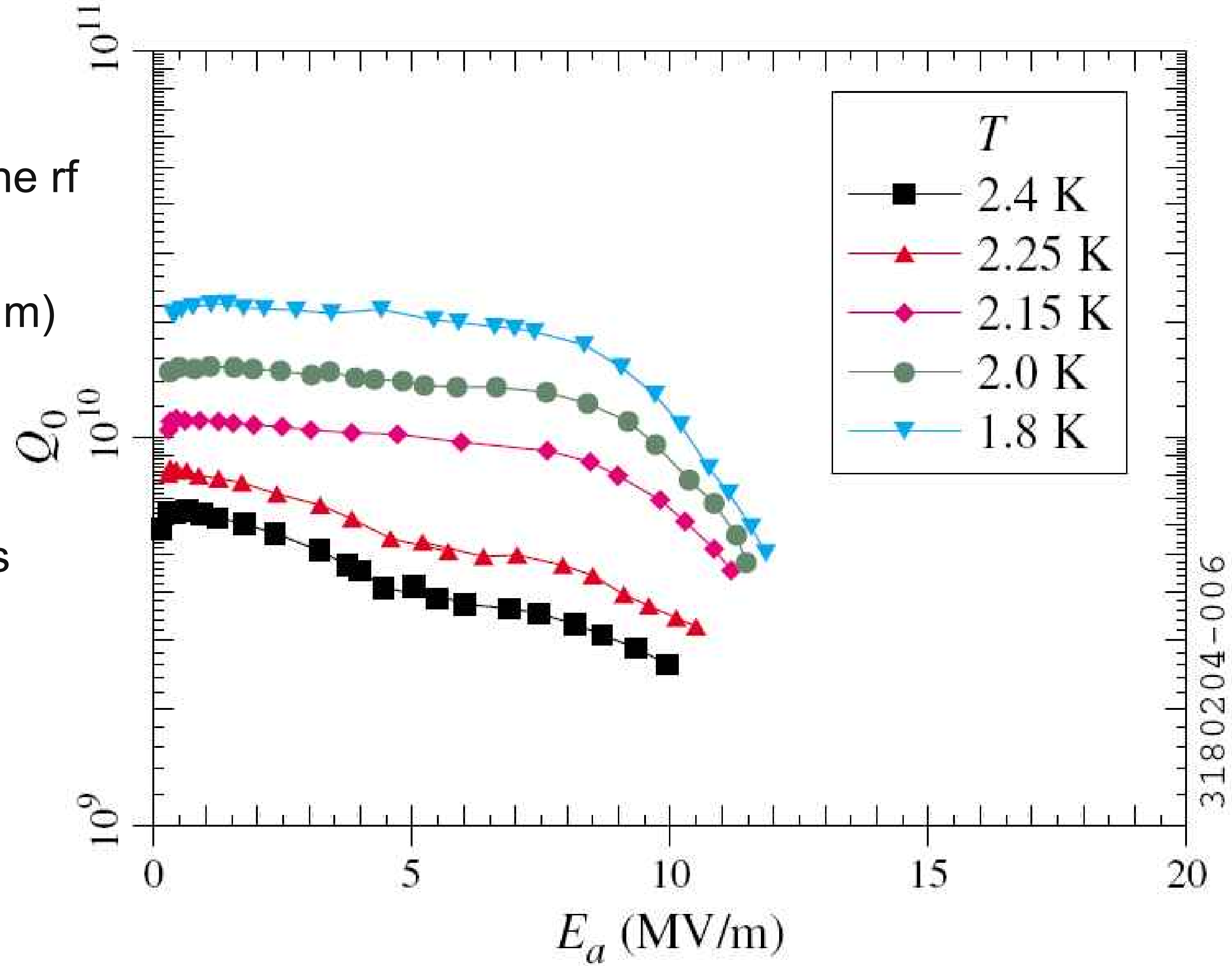

FIG. 9. (Color) Measured dependence of the quality factor on the accelerating gradient at different bath temperatures for the first 6-cell cavity prototype (January 2003).

Thermal Properties of Cavities

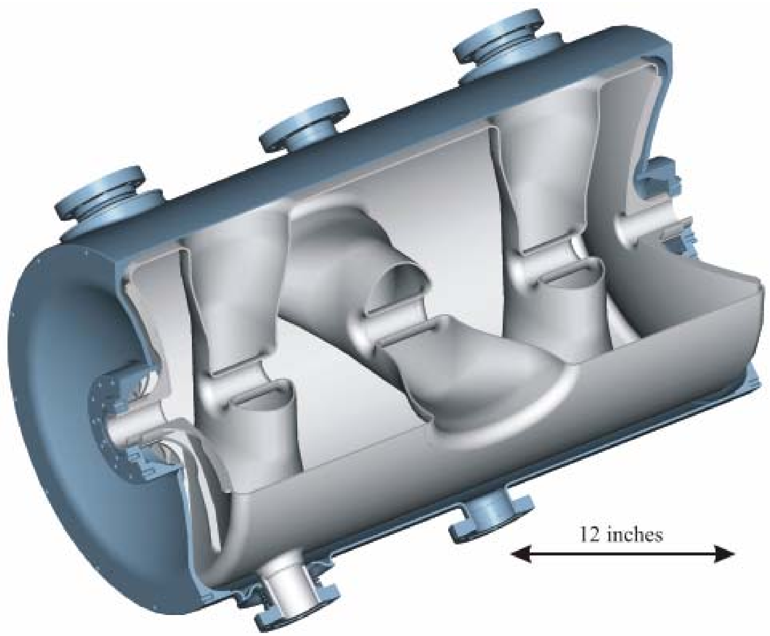

Total Heat Capacity (J/K)		
	293 K	4.2 K
He	20	15000
Nb	13600	22

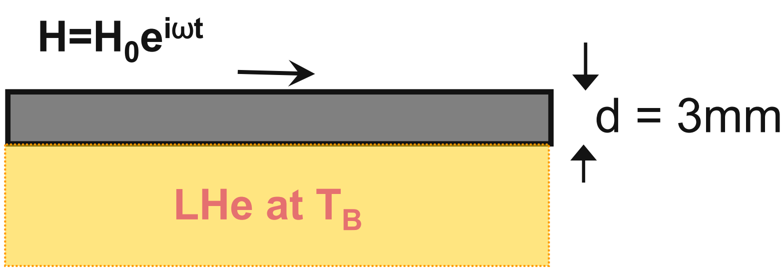

Thermal Relaxation Time (3mm sheet)		
	293 K	4.2 K
Nb	200 msec	.03-0.3 msec

Thermal-magnetic Breakdown

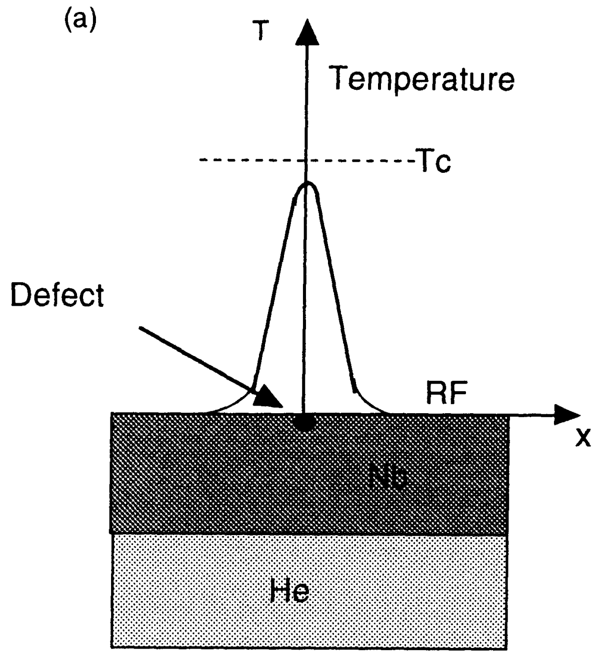

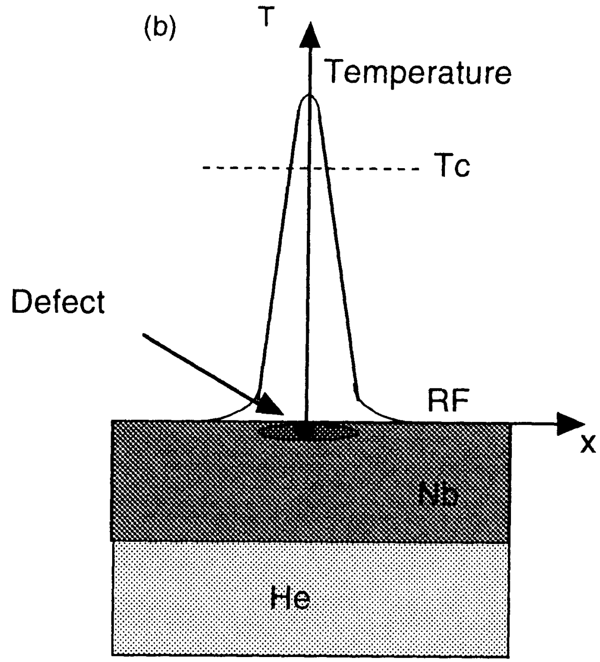

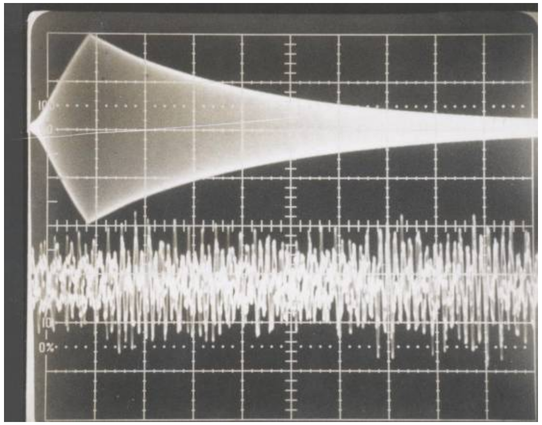

SC cavity being pulsed to a high field level. Horizontal scale is 5 msec/div

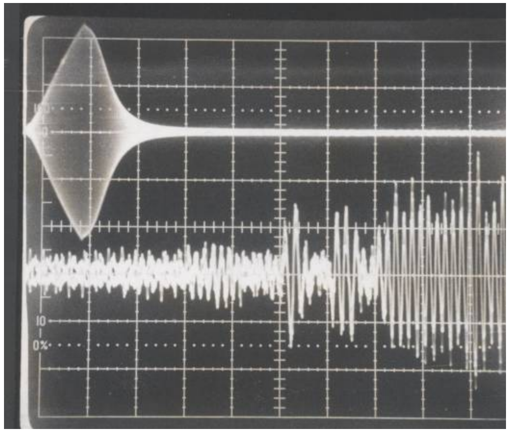

Thermal Stability and RRR

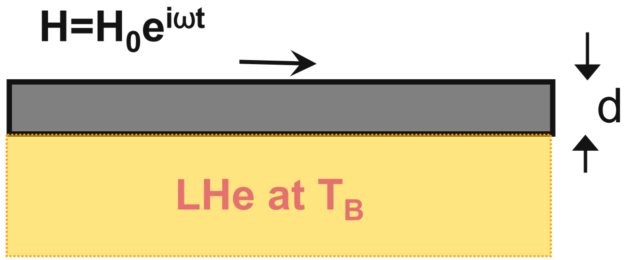

Is a normal region unstable?

I.e. is the temperature rise $\delta T < (T_C\text{-}T)$

given by $\delta T = d \cdot ½ R_S \cdot H_M^2 / K_{eff}$, ***where***

$K_{eff} = \int K \cdot dT/(T2\text{-}T1)$, ***so the maximum stable field is given by***

$H_M^2 = 2 \cdot d \cdot (T_C\text{-}T_B) \cdot (1/K_{eff} \cdot R_S)$

Note that $R_S \sim \omega^{½}$ so that

$H_M \sim \omega^{-¼}$

And thermal stability is better at lower frequencies

At 1 GHz and 2 K the limit is 50-500 G depending on the purity of the material

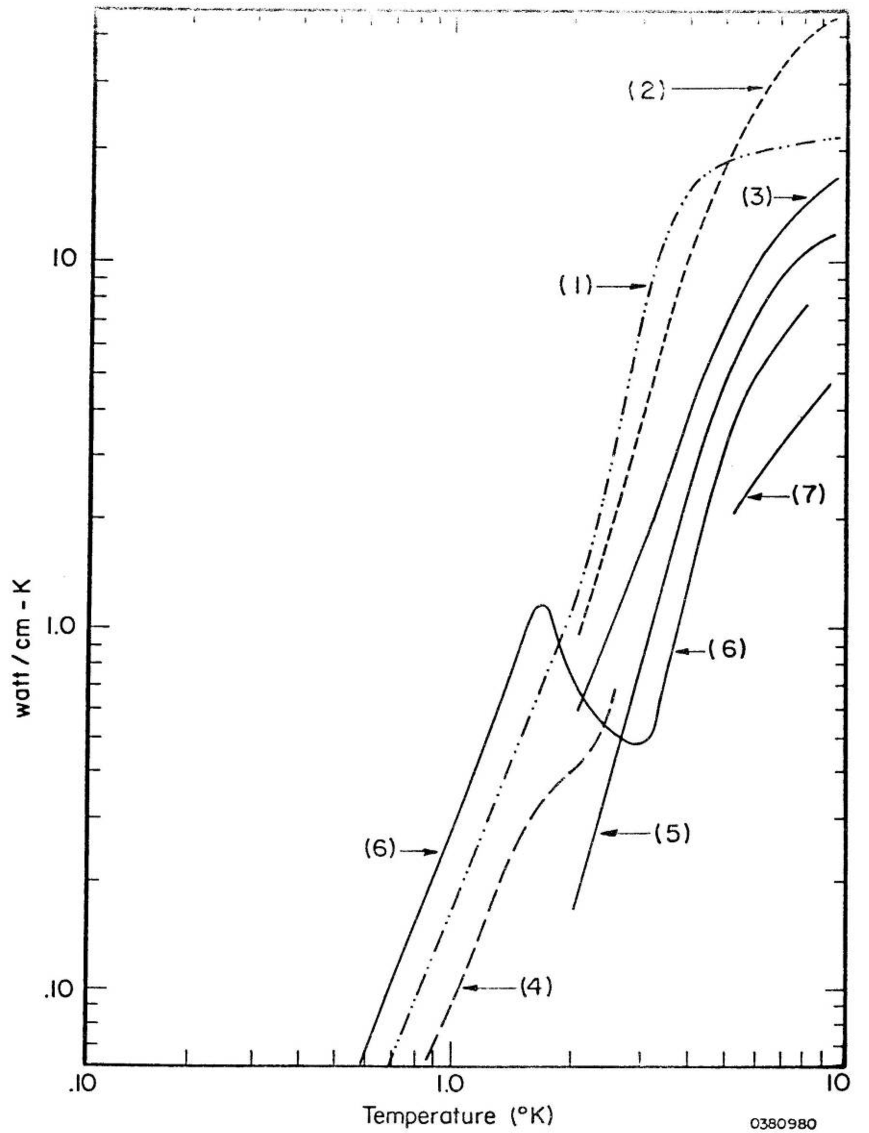

Fig. 2A: Thermal conductivity of Nb in the superconducting state: samples of highest purity. Refer to the key on page 19 to identify the curves.

High-pressure water rinsing gives a dramatic improvement

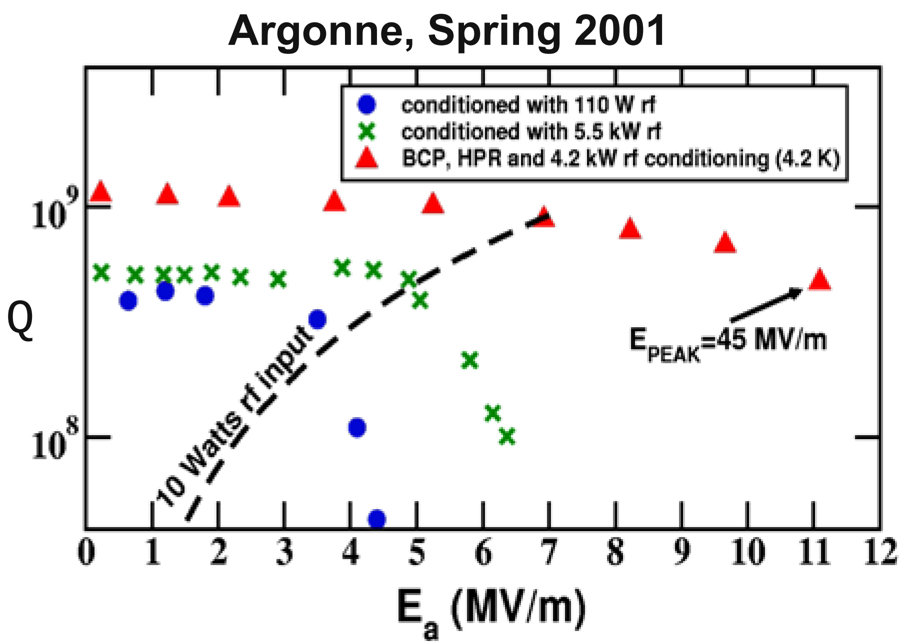

Electropolished Nb Surface

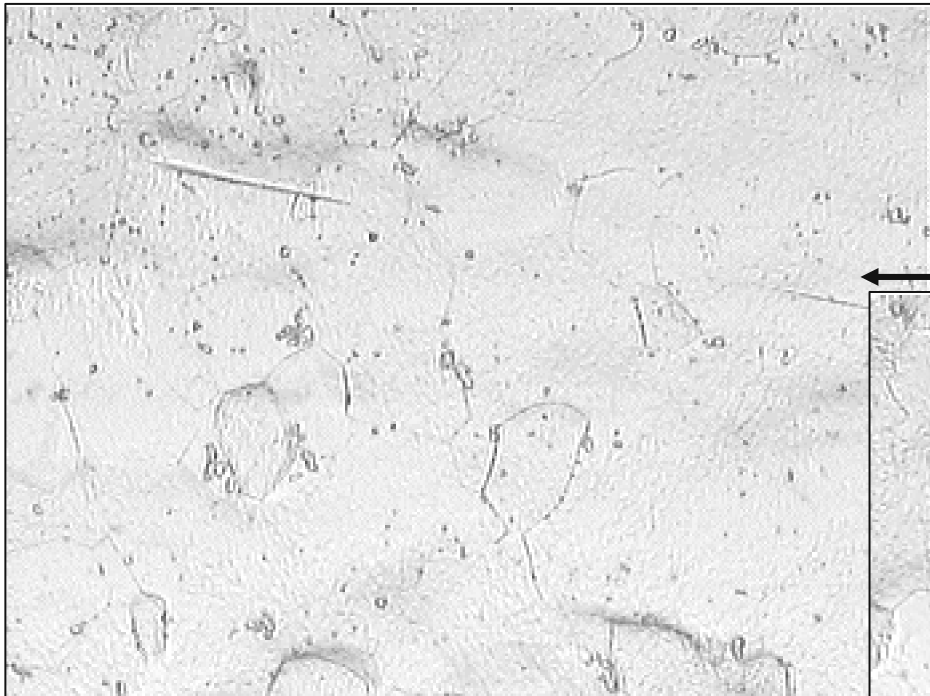

Cleaned with ethanol and
Acetone, before HPR

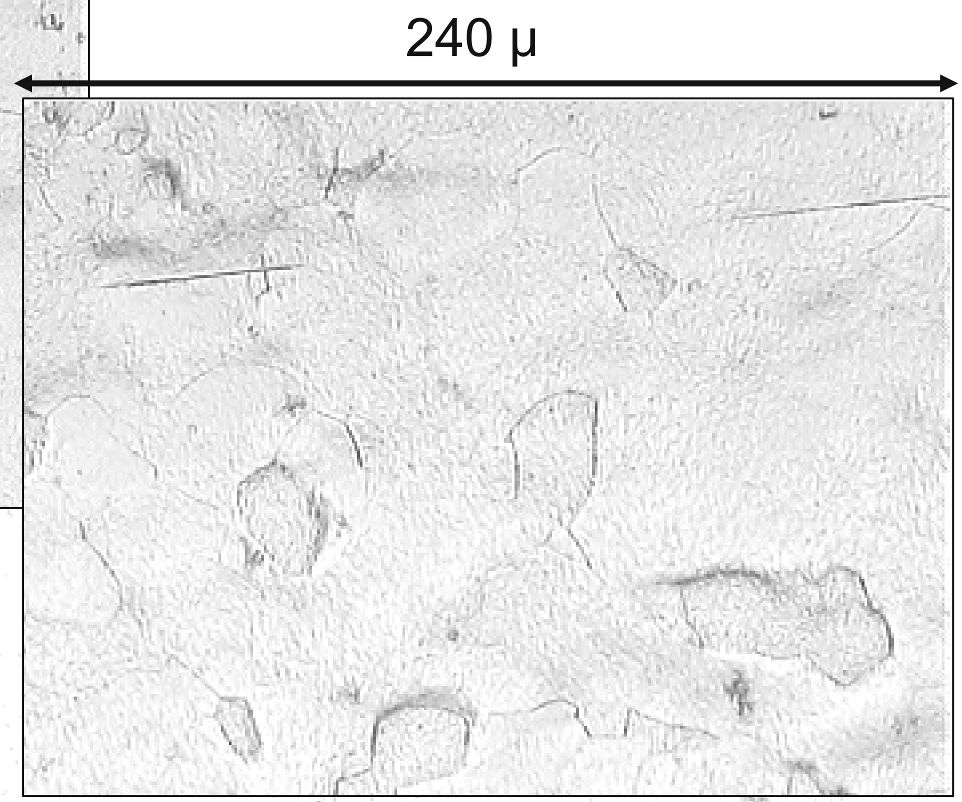

After HPR at 1750 PSI

Mechanical properties – frequency and phase control

Lorenz Detuning

$\Delta f = K_L \bullet E_A^2$

Typically K_L = 1-10 Hz/(MV/m)^2

A physical picture is a can full of a photon gas. Radiation pressure expands the can, doing negative work on the photons, so the frequency drops:

Boltzmann-Ehrenfest

Work = U • Δω/ω

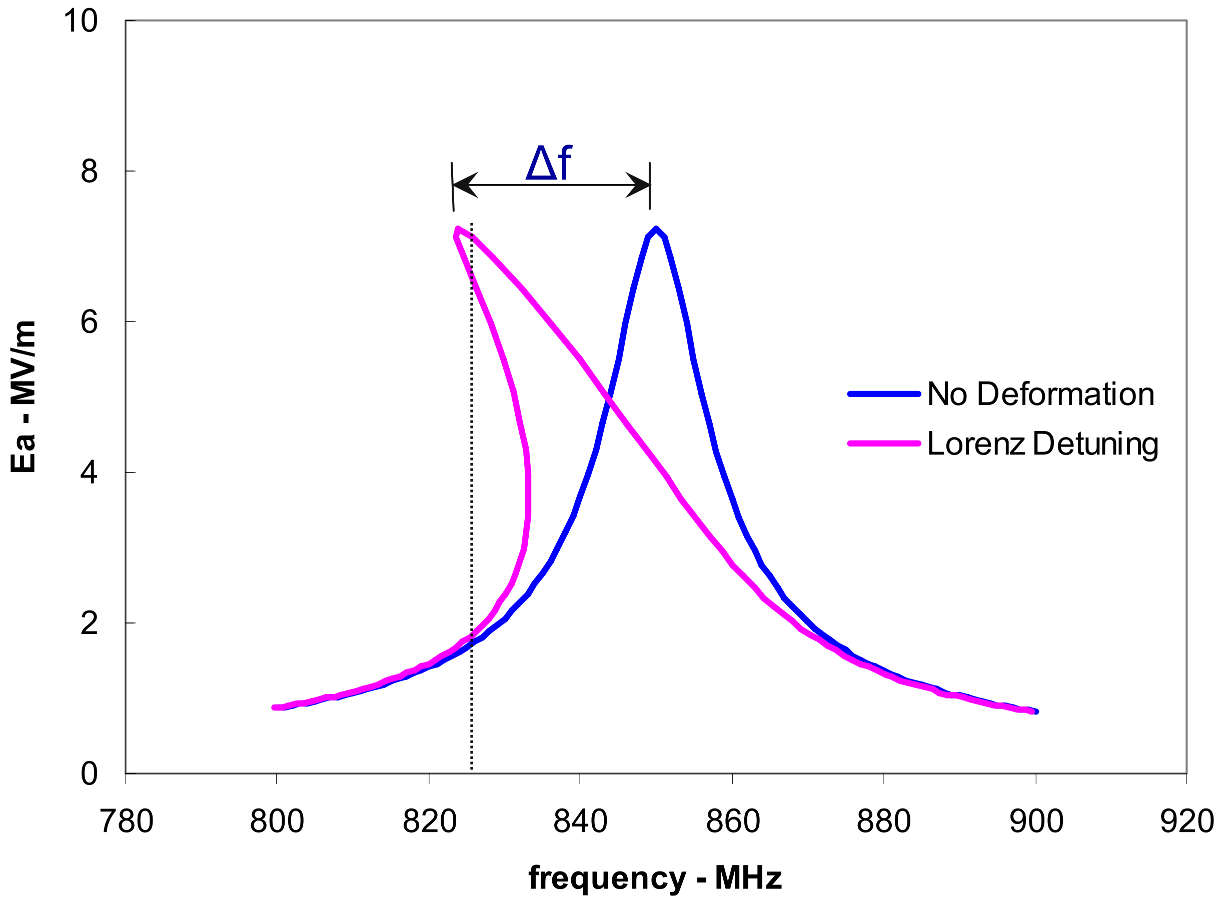

Microphonics are a **Big Issue** *for SC Cavities with Moderate Beam-loading (operating cw)*

Tuner must switch rf power given by:

$$P = (U_0 \bullet E_A^2) \bullet \delta\omega_{p\text{-}p}$$

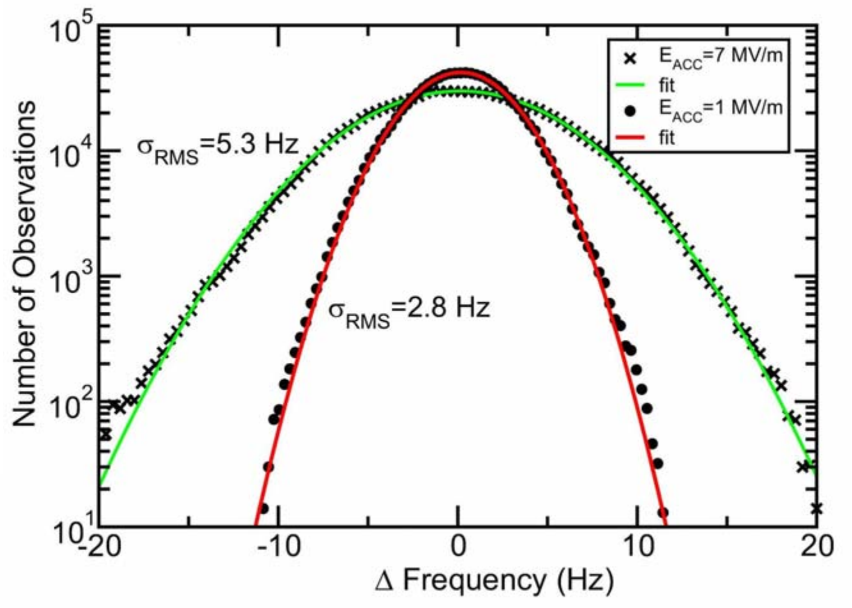

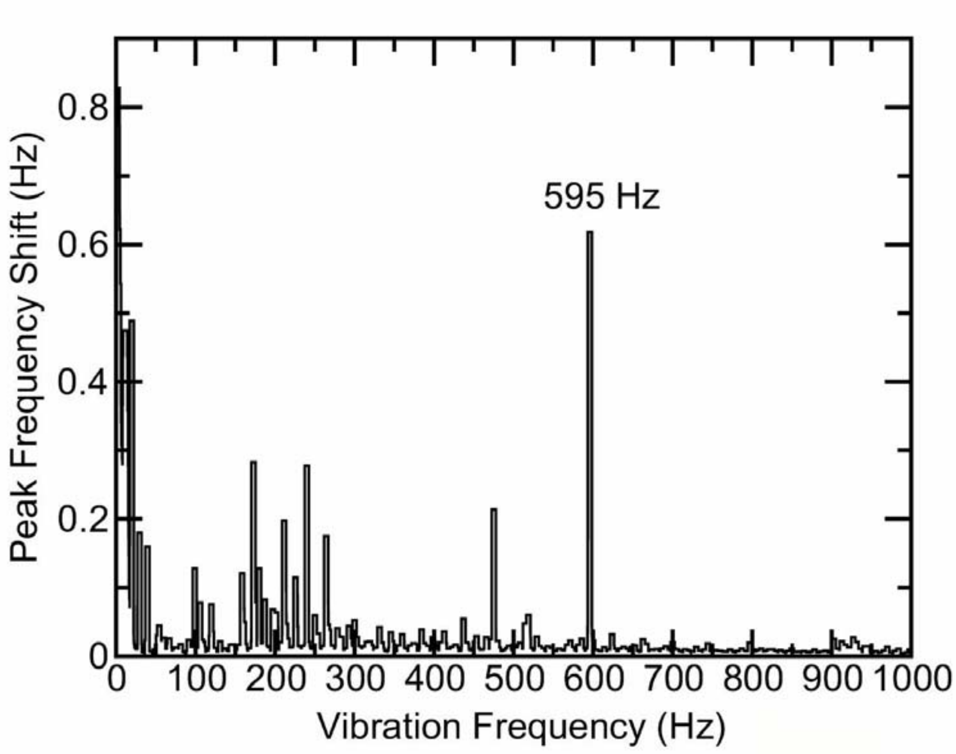

Microphonic Phase-noise in the 345 MHz Double-spoke cavity

Cavity Fabrication

Building a high-performance nb cavity is an utterly unforgiving process. Very small defects (cracks, fissures, inclusions, weld-spatter) are difficult to diagnose, and can destroy performance.

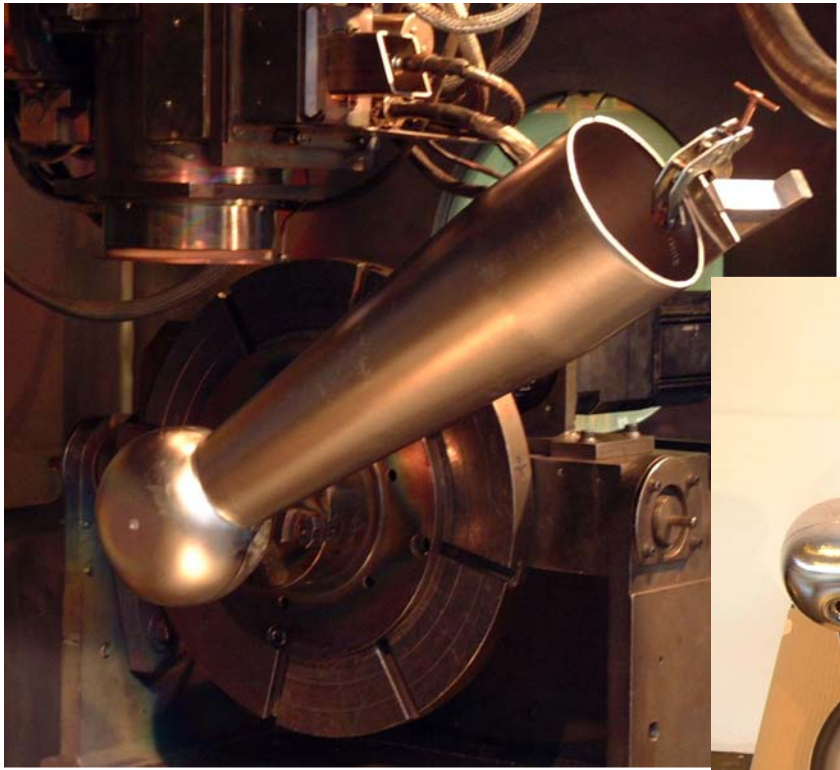

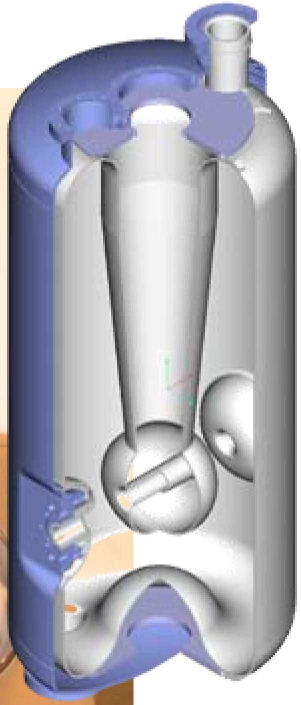

After fabrication, a hundred microns of nb surface must be chemically removed to eliminate defects

A good cavity is just the start – couplers, tuners, and cryostats are all critical elements of a SC accelerator

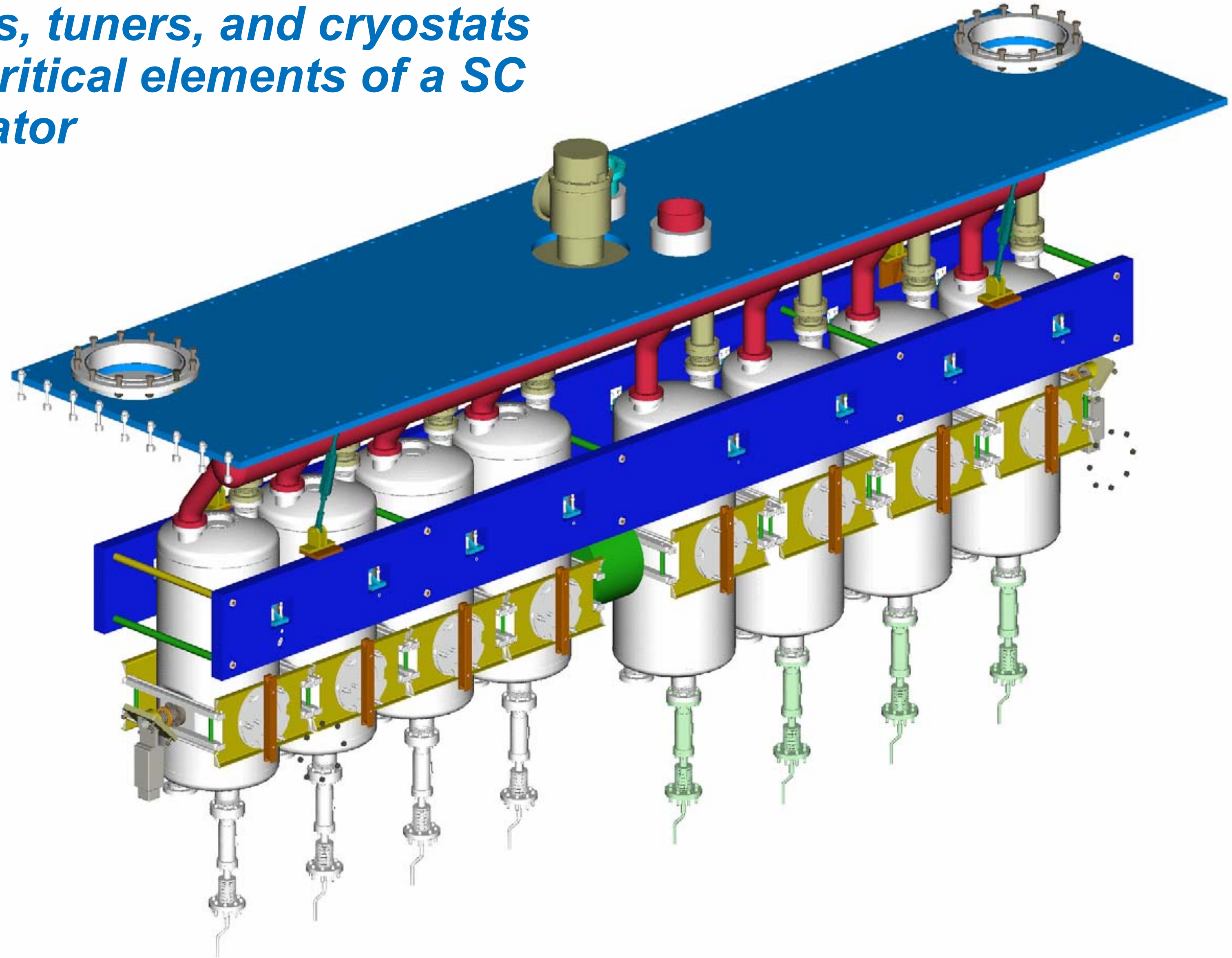

What is present state-of-the-art

- Very high purity bulk niobium, typically 3mm sheet is the material of choice (RRR > 200 and up, depending on frequency)
- Achievable peak surface electric fields are approaching 100 MV/m – this requires the most stringent low-particulate conditions and whether this performance can be maintained operationally remains to be seen
- Peak surface magnetic fields of more than 1000 G over significant surface areas have been achieved – this requires the number and size of defects to be exceedingly small over large areas of cavity surface.
- We are near the limits of niobium (after 40 years of R&D). Any substantial further gains in performance will require the development of other materials (Nb_3Sn would be my choice: x2.5 in magnetic field)

Follow-on talks:

- June 8 – Mike Kelly will discuss surface processing, ultra-clean techniques: the major performance-determining aspects of SRF technology

- June 15 – Zach Conway will discuss Lorenz detuning, microphonics, tuners, couplers, and describe the process of cold-testing

- Date to be determined – Joel Fuerst will discuss refrigeration, cryostats, and cavity construction and assembly